

## Spatially correlated diversity-induced resonance

Dan Wu,<sup>\*</sup> Shiqun Zhu,<sup>†</sup> and Xiaoqin Luo

*School of Physical Science and Technology, Suzhou University, Suzhou, Jiangsu 215006, People's Republic of China*

(Received 25 September 2008; published 6 May 2009)

Based on recent work [C. J. Tessone, C. R. Mirasso, R. Toral, and J. D. Gunton, *Phys. Rev. Lett.* **97**, 194101 (2006)], the study of coupled bistable oscillators with different sources of diversity is extended. Effects of the correlation between the diversity on the resonant response of the system are discussed. It is found that the diversity of the coupled system, in the form of quenched noise, can induce a resonant effect in response to external signals. The resonance is reduced and even disappears as the correlation length between the diversity increases, while the spatial synchronization is enhanced due to the correlation between the diversity.

DOI: [10.1103/PhysRevE.79.051104](https://doi.org/10.1103/PhysRevE.79.051104)

PACS number(s): 02.50.-r, 05.45.Xt

### I. INTRODUCTION

In the last decades, stochastic resonance has been investigated extensively due to its potential applications [1–6]. It is well known that the noise in the system has a constructive role on stochastic resonance. The response of the system to an external signal may show a resonantlike behavior at an optimal noise strength. In recent years, the investigation of stochastic resonance was extended to the coupled oscillator system. For example, Lindner *et al.* [7] found the phenomenon of array-enhanced stochastic resonance (AESR) in a coupled system. Zhou *et al.* [8] found the array-enhanced coherence resonance (AECR) in an array of coupled FitzHugh-Nagumo neurons.

Recently, Tessone *et al.* [9] pointed out that the right amount of diversity, in the form of quenched noise, can induce a resonant collective behavior in an ensemble of  $N$  globally coupled bistable systems. The independent diversity with different sources between the coupled oscillators can play a constructive role on the resonant response of the coupled system to an external periodic force. However, in certain situations the diversity may have a common origin and then may be correlated [10–15]. Therefore, the effects of the correlation between the diversity on the behavior of the system need to be further investigated.

In this paper, the phenomena of diversity-induced resonance in an array of coupled bistable oscillators are investigated when there exists mutual correlation in the diversity parameter. In Sec. II, the dynamical model of the coupled bistable system with correlated diversity is presented. In Sec. III, the effects of the correlation  $\lambda$  between the diversity and the coupling  $c$  between different oscillators on the resonant response and the spatial synchronization of the coupled system are discussed. A discussion concludes the paper.

### II. DYNAMICAL MODEL

The ensemble of  $N$  coupled bistable oscillators with correlated diversity can be written as follows:

$$\dot{x}_i(t) = x_i(t) - x_i^3(t) + a_i + A \sin(\Omega t) + \frac{c}{N} \sum_{j=1}^N [x_j(t) - x_i(t)], \quad (1)$$

where  $A$  is the amplitude of the external periodic signal,  $\Omega = 2\pi/T$  is the frequency of the signal, and  $c$  is the coupling strength between oscillators. The parameter  $a_i$  is assumed to take short-range correlated diversity with the following statistical properties:

$$\langle a_i \rangle = 0, \quad \langle a_i a_j \rangle = g(|i - j|),$$

$$g(|i - j|) = g(0) \exp\left[-\frac{|i - j|^2}{2\lambda^2}\right], \quad (2)$$

$$g(0) = \frac{\varepsilon}{\lambda\sqrt{2\pi}}, \quad (3)$$

where  $\varepsilon$  is the diversity and  $\lambda$  is correlation of the diversity between a pair of elements. In the limit of  $\lambda \rightarrow 0$ , it is possible to recover the independent diversity shown in Ref. [9].  $a_i$  are Gaussian variables and the correlation functions of  $a_i$  depend on the distance  $|i - j|$  between the sites in a one-dimensional space. For each lattice point  $i$ , the diversity parameter  $a_i$  takes a different value, but constant in time. The actual algorithm for the generation of the correlated variables is presented in the Appendix.

### III. EFFECTS OF CORRELATION BETWEEN DIVERSITY ON DIVERSITY-INDUCED RESONANCE

To investigate the response of the periodically driven system, the spectral amplification factor [9]  $\eta = 4A^{-2} \langle |e^{i\Omega t} X(t)|^2 \rangle$  is calculated, where  $X(t) = \frac{1}{N} \sum_{i=1}^N x_i(t)$  is the average position of the oscillators at time  $t$ . The spectral amplification factor can provide a precise amount of the information in the signal transported with a particular forcing period.

The spectral amplification factor  $\eta$  is plotted in Fig. 1 as a function of the diversity  $\varepsilon$  and the coupling strength  $c$ . A three-dimensional plot of the spectral amplification factor  $\eta$  is shown in Fig. 1(a). From Fig. 1(a), it is seen that the amplification factor  $\eta$  is a nonmonotonic function of diver-

<sup>\*</sup>wud@suda.edu.cn

<sup>†</sup>szhu@suda.edu.cn

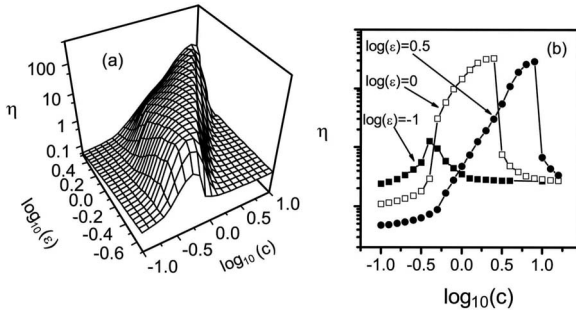


FIG. 1. Spectral amplification factor  $\eta$  of the coupled bistable system is plotted as a function of the diversity  $\varepsilon$  and the coupling strength  $c$ . The parameters are chosen as  $N=1000$ ,  $A=0.2$ ,  $T=10^3$ , and  $\lambda=1$ . (a) Three-dimensional plot of  $\eta$ . (b)  $\eta$  is plotted as a function of  $\log_{10}(c)$ .

sity  $\varepsilon$ . There exists an optimal value of  $\varepsilon$ , which is the characteristic signature of stochastic resonance. There also exists an optimal coupling strength  $c$ , which is the main results of AESR [7].  $\eta$  is plotted in Fig. 1(b) as a function of  $\log_{10}(c)$  when  $\varepsilon$  is varied. From Fig. 1(b), it is clear that the optimal value is shifted to a large value of the coupling strength  $c$  when the diversity  $\varepsilon$  is increased. The mechanism can be understood as follows. In the homogeneous case, that is  $a_i=0$ , the subthreshold forcing cannot overcome the potential barrier for any of them. As the diversity increases, a number of elements with certain value of  $a_i$  are able to overcome the potential barrier with the help of external forcing. The coupling between the elements can help these elements to pull the other elements and produce a collective, macroscopic movement. However, if the coupling is too strong, the system becomes globally synchronized. The coupled system may behave as a single element. The typical effect of array-enhanced resonance disappears [7,8]. There exists an optimal coupling strength. For too large diversity, some of the elements pulled by diversity offer too much resistance to follow the external force. Larger coupling strength is needed for the favorable elements to overcome the resistant effects. Therefore, the optimal value of  $\eta$  is shifted to a large value of the coupling strength  $c$  when the diversity  $\varepsilon$  is increased.

When the correlation length  $\lambda$  is small, the spectral amplification factor  $\eta$  is plotted in Fig. 2 as a function of the diversity  $\varepsilon$  and the correlation length  $\lambda$ . A three-dimensional plot of  $\eta$  is shown in Fig. 2(a). It is found that the amplification factor  $\eta$  is a nonmonotonic function of diversity  $\varepsilon$ . The maximum value of  $\eta(\eta_{\max})$  as a function of  $\lambda$  is plotted in Fig. 2(b). When  $\lambda$  is increased,  $\eta_{\max}$  decreases almost

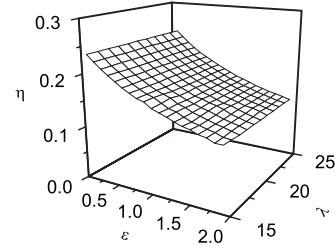


FIG. 3. Spectral amplification factor  $\eta$  of the coupled bistable system is plotted as a function of the diversity  $\varepsilon$  and the correlation length  $\lambda$  when  $\lambda$  is very large.

linearly with  $\lambda$ . That is, the increase of the correlation length  $\lambda$  can reduce the height of  $\eta$ . The optimal value  $\varepsilon_{\text{opt}}$  corresponding to  $\eta_{\max}$  as a function of  $\lambda$  is plotted in Fig. 2(c). From Fig. 2(c), it is seen that  $\varepsilon_{\text{opt}}$  increases almost linearly as  $\lambda$  increases. That is, the position of the peak shifts to a larger value of  $\varepsilon$  when the correlation length is increased. It means that the correlation between the diversity may reduce the resonant effect that is induced by diversity. Thus the maximum value of  $\eta$  is decreased and a larger diversity is needed to overcome the passive effects induced by the correlation  $\lambda$ .

The spectral amplification factor  $\eta$  is plotted in Fig. 3 as a function of the diversity  $\varepsilon$  and the correlation length  $\lambda$  when the correlation length  $\lambda$  is very large. It is found that the amplification factor  $\eta$  is decreased monotonically as a function of the diversity  $\varepsilon$ . The value of  $\eta$  does not change very much when  $\lambda$  is increased. That is to say, when the correlation between the diversity is very large, the signature of stochastic resonance disappears.

It is well known that coupled oscillators are able to synchronize. When the short-range spatial diversity is considered, the synchronization behavior can be investigated by the mean-square deviation [16]. Comparing Figs. 2 and 3 to Fig. 1, it is found that the effect of the correlation length  $\lambda$  on the resonant behavior is different to that of the coupling strength  $c$ . The resonance phenomena show the temporal order of the system output [17]. In order to investigate the spatial order of the system, the degree of spatial synchronization can be calculated [17]. The cooperative effects caused by the diversity  $\varepsilon$ , the correlation length  $\lambda$ , and the coupling strength  $c$  on the spatial synchronization need to be investigated. To characterize the synchronization, the mean-square deviation can be calculated [16]

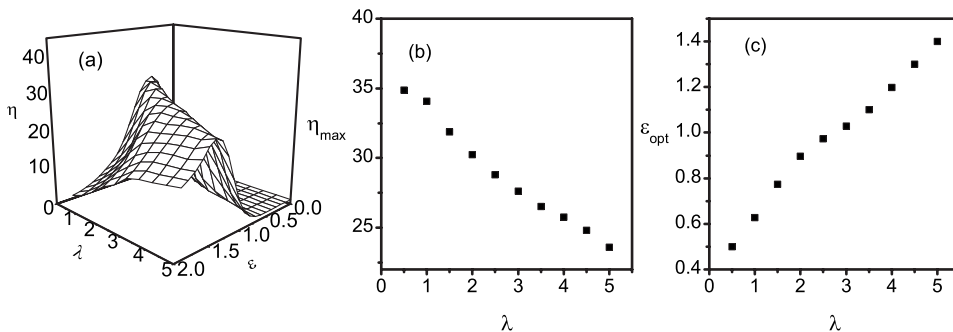


FIG. 2. (a) Spectral amplification factor  $\eta$  of the coupled bistable system is plotted as a function of the diversity  $\varepsilon$  and the correlation length  $\lambda$  between the diversity. (b) The maximum value of  $\eta_{\max}$  is plotted as a function of  $\lambda$ . (c) The optimal value of  $\varepsilon_{\text{opt}}$  is plotted as a function of  $\lambda$ . The parameters are chosen as  $N=1000$ ,  $A=0.2$ ,  $T=10^3$ , and  $c=1$ .

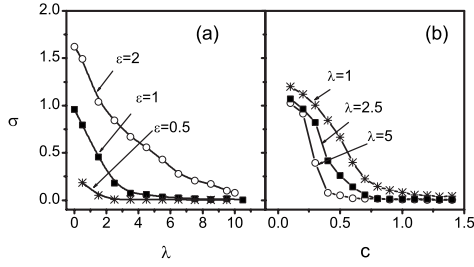


FIG. 4. (a) The mean-square deviation  $\sigma$  as a function of the correlation length  $\lambda$  for different values of diversity  $\epsilon$ . The parameters are chosen as  $N=1000$ ,  $A=0.2$ ,  $T=10^3$ , and  $c=1$ . (b) The mean-square deviation  $\sigma$  as a function of the coupling strength  $c$  for different values of  $\lambda$ . The parameters are chosen as  $N=1000$ ,  $A=0.2$ ,  $T=10^3$ , and  $\epsilon=0.5$ .

$$\sigma^2 = \frac{1}{N} \left\langle \sum_{i=1}^N [x_i(t) - \langle x \rangle]^2 \right\rangle_t, \quad (4)$$

where  $\langle x \rangle$  denotes an average over the elements of the array and refers to  $\langle x \rangle = \frac{1}{N} \sum_{i=1}^N x_i(t)$  while  $\langle \dots \rangle_t$  denotes an average over time. Large  $\sigma$  represents large deviations between various oscillators and small  $\sigma$  denotes strong collective motion and, consequently, better synchronization. Extremely,  $\sigma=0$  demonstrates complete synchronization [17,18].

The mean-square deviation  $\sigma$  as a function of the correlation length  $\lambda$  and the coupling strength  $c$  is plotted in Fig. 4. In Fig. 4(a),  $\sigma$  is plotted as a function of  $\lambda$  for different values of diversity  $\epsilon$ . It is found that  $\sigma$  always decreases monotonically as  $\lambda$  increases, which means the spatial synchronization is improved due to the correlation between the diversity. It is easier for the system with small diversity to reach complete synchronization with the help of the correlation between the diversity. In Fig. 4(b),  $\sigma$  is plotted as a function of  $c$  for different values of  $\lambda$ . It is found that the spatial synchronization is improved due to the coupling between the oscillators. The correlation between the diversity may reinforce the synchronization.

From the above discussions, it is seen that the diversity-induced resonance and the spatial synchronization appear for different parameter regimes in coupled bistable oscillators with correlated diversity. For small correlation length  $\lambda$ , the diversity-induced resonance appears while the synchronization in the system is quite poor. For large correlation length  $\lambda$ , the diversity-induced resonance may disappear while the synchronization is enhanced and complete synchronization may occur. That is, the correlation length  $\lambda$  has opposite effect on diversity resonance and the synchronization. For suitable value of the coupling  $c$ , both the diversity-induced resonance and the synchronization may occur. These phenomena may be enhanced by increasing the coupling  $c$ .

#### IV. DISCUSSION

The phenomena of diversity-induced resonance in a coupled bistable oscillators are investigated when there exists mutual correlation in the diversity parameter. The effects of coupling  $c$  between oscillators and the correlation length  $\lambda$

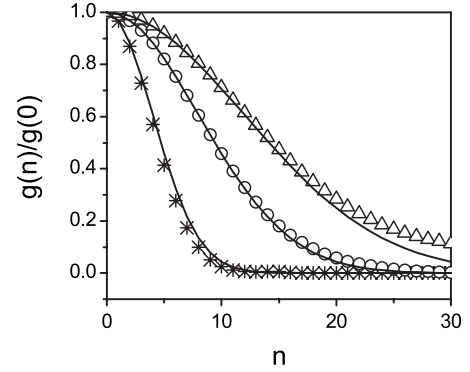


FIG. 5. The correlation function  $g(n)/g(0)$  of spatial disorder is plotted as a function of  $n$  for different values of correlation length  $\lambda$ . Solid lines are theoretical results and the symbols are numerical calculations with  $\lambda=4$ (\*),  $8$ ( $\circ$ ),  $12$ ( $\triangle$ ).

between the diversity on the resonant response of the system are discussed. It is found that increasing the correlation length  $\lambda$  can reduce the resonance. While increasing the coupling  $c$  between oscillators can enhance the resonance. The signature of stochastic resonance even disappears when the correlation length between the diversity is very large. Both the coupling between oscillators and the correlation between the diversity can enhance the spatial synchronization of the system. Our findings may be of importance to speculate the amount of diversity and the correlation between diversity present in some neurobiology system, such as the FitzHugh-Nagumo model [9], the Hindmarsh-Rose (HR) model [19], the Hodgkin-Huxley model [20,21], and the Morris-Lecar model [22], etc.

#### ACKNOWLEDGMENTS

Financial supports from the National Natural Science Foundation of China (Grant No. 10847156) and the Natural Science Foundation of Jiangsu Province of China (Grant No. BK2001138) are gratefully acknowledged.

#### APPENDIX

The actual algorithm for the generation of the correlated variables is presented as follows. In the  $\omega$ -Fourier space, the correlation of Eq. (2) reads [23,24]

$$\langle a(\omega)a(\omega') \rangle = 2\pi g(\omega)\delta(\omega + \omega'), \quad (A1)$$

where  $a(\omega)$ ,  $a(\omega')$ , and  $g(\omega)$  are the Fourier transforms of  $a_i$ ,  $a_j$ , and  $g_i$ , respectively. The motion will take place in a one-dimensional space discretized in  $N$  cells of size  $\Delta L$ . Every one of these intervals will be denoted by a Roman index in real space and by a Greek index in Fourier space. So the discrete Fourier version of Eq. (A1) is given by

$$\langle a(\omega_\mu)a(\omega_{\mu'}) \rangle = N\Delta L g(\omega_\mu)\delta_{\mu+\mu',0}. \quad (A2)$$

Then the noise in the Fourier space can be constructed as

$$a(\omega_\mu) = \sqrt{N\Delta L g(\omega_\mu)} \xi(\omega_\mu), \quad (\mu = 0, \dots, N-1),$$

$$a(\omega_0) = a(\omega_N), \quad \omega_\mu = \frac{2\pi\mu}{N\Delta L}, \quad (\text{A3})$$

where  $\xi(\omega_\mu) \equiv \xi_\mu$  are Gaussian random numbers with zero mean and correlation

$$\langle \xi_\mu \xi_\nu \rangle = \delta_{\mu+\nu,0}, \quad (\text{A4})$$

$\xi_\mu$  is a complex variable and can be constructed as  $\xi_\mu = b_\mu + id_\mu$ , and  $b_\mu$  and  $d_\mu$  represent Gaussian random numbers with zero mean and variances

$$\langle b_0^2 \rangle = 1, \quad \langle d_0^2 \rangle = 0,$$

$$\langle b_\mu^2 \rangle = \langle d_\mu^2 \rangle = \frac{1}{2}, \quad (\mu = 1, 2, \dots, N-1). \quad (\text{A5})$$

The discrete inverse transform of  $a(\omega_\mu)$  is then numerically calculated by a fast Fourier transform algorithm. Thus, a string of  $N$  numbers  $a_i$  is generated.

In order to check the suitability of the procedure, the correlation of Eq. (2) is numerically evaluated by

$$g(n) = \left\langle \frac{\sum_{i=0}^{N_0} a_{i+n} a_i}{N_0 + 1} \right\rangle, \quad (n = 0, 1, 2, \dots), \quad (\text{A6})$$

where the number of the network is  $N=2^{22}$  and  $N_0=N/4$  and  $\Delta L=0.01$  are used in the simulation.

To check the algorithm for the generation of the random numbers, the numerical results and the theoretical predictions of the spatial correlation function  $g(n)/g(0)$  against  $n$  for different values of the correlation length  $\lambda$  are plotted in Fig. 5. The lines are theoretical predictions of Eq. (3) while the symbols are numerical results. For very large values of  $\lambda$ , there is a small amount of deviations between numerical computations and theoretical results when  $n$  is very large. This deviation is mainly caused by the periodic boundary conditions in the process of the discrete Fourier transform [23]. For small and medium values of  $\lambda$ , the numerical computations are in excellent agreement with the theoretical results. From the whole shape of the curve, the numerical simulations can still characterize the theoretical curve quite well [1]. This assures the reliability of the numerical algorithm when  $\lambda$  is not very large.

- 
- [1] R. Benzi, G. Parisi, A. Suter, and A. Vulpiani, *J. Phys. A* **14**, L453 (1981).
- [2] J. Douglass, L. Wilkens, E. Pantazelou, and F. Moss, *Nature (London)* **365**, 337 (1993).
- [3] K. Wiesenfeld and F. Moss, *Nature (London)* **373**, 33 (1995).
- [4] L. Gammaitoni, P. Hänggi, P. Jung, and F. Marchesoni, *Rev. Mod. Phys.* **70**, 223 (1998).
- [5] A. A. Zaikin, J. Kurths, and L. Schimansky-Geier, *Phys. Rev. Lett.* **85**, 227 (2000).
- [6] E. I. Volkov, E. Ullner, A. A. Zaikin, and J. Kurths, *Phys. Rev. E* **68**, 026214 (2003).
- [7] J. F. Lindner, B. K. Meadows, W. L. Ditto, M. E. Inchiosa, and A. R. Bulsara, *Phys. Rev. Lett.* **75**, 3 (1995).
- [8] C. Zhou, J. Kurths, and B. Hu, *Phys. Rev. Lett.* **87**, 098101 (2001).
- [9] C. J. Tessone, C. R. Mirasso, R. Toral, and J. D. Gunton, *Phys. Rev. Lett.* **97**, 194101 (2006).
- [10] A. J. R. Madureira, P. Hänggi, and H. S. Wio, *Phys. Lett. A* **217**, 248 (1996).
- [11] A. Fulinski and T. Telejko, *Phys. Lett. A* **152**, 11 (1991).
- [12] Y. Jia, X.-P. Zheng, X.-M. Hu, and J.-R. Li, *Phys. Rev. E* **63**, 031107 (2001).
- [13] X. Luo and S. Zhu, *Phys. Rev. E* **67**, 021104 (2003).
- [14] K. P. Singh, G. Ropars, M. Brunel, and A. Le Floch, *Phys. Rev. A* **73**, 033807 (2006).
- [15] K. Lü and J. D. Bao, *Phys. Rev. E* **72**, 067701 (2005).
- [16] C. Masoller and A. C. Marti, *Phys. Rev. Lett.* **94**, 134102 (2005).
- [17] Z. Gao, B. Hu, and G. Hu, *Phys. Rev. E* **65**, 016209 (2001).
- [18] Q. Wang, Z. Duan, M. Perc, and G. Chen, *Europhys. Lett.* **83**, 50008 (2008).
- [19] J. P. Baltanás and J. M. Casado, *Phys. Rev. E* **65**, 041915 (2002).
- [20] A. Longtin, *Phys. Rev. E* **55**, 868 (1997).
- [21] S.-G. Lee, A. Neiman, and S. Kim, *Phys. Rev. E* **57**, 3292 (1998).
- [22] P. Balenzuela, J. M. Buldú, M. Casanova, and J. Garcia-Ojalvo, *Phys. Rev. E* **74**, 061910 (2006).
- [23] A. H. Romero and J. M. Sancho, *Phys. Rev. E* **58**, 2833 (1998).
- [24] J. Garcia-Ojalvo and J. M. Sancho, *Noise in Spatially Extended System* (Springer-Verlag, New York, 1999).